Published in IET Optoelectronics
Received on 20th June 2013
Revised on 29th August 2013
Accepted on 6th September 2013
doi: 10.1049/iet-opt.2013.0078

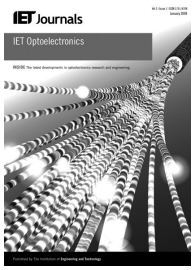

ISSN 1751-8768

Analysis of frequency chirp of self-injected nanostructure semiconductor lasers

Cheng Wang[1,2], Jacky Even[2], Frederic Grillot[1]

[1]*Laboratoire CNRS LTCI, Ecole Nationale Supérieure des Télécommunications, Télécom ParisTech, 46 rue Barrault, 75634 Paris Cedex, France*
[2]*Laboratoire CNRS FOTON, INSA, Université Européenne de Bretagne, 20, avenue des buttes de Coësmes, 35043 Rennes Cedex, France*
E-mail: frederic.grillot@telecom-paristech.fr

Abstract: The frequency chirp of a self-injected quantum dot (QD) semiconductor laser is studied through the chirp-to-power ratio. By taking into account the carrier dynamics in the nanostructures, the effects of the optical feedback conditions as well as of the linewidth enhancement factor are investigated with a semi-analytical rate equation model. On the one hand, under the long delay case, the simulations show the occurrence of a detrimental parasitic ripple both in the amplitude and the frequency responses. On the other hand, in the short cavity regime, the calculations reveal that the modulation properties can be nicely purified regarding the amplitude and the phase of the delayed field. To this end, substantial improvements in terms of the modulation bandwidth, the relaxation frequency and the frequency chirp are pointed out. Finally, the simulations also show that the linewidth enhancement factor constitutes a severe constraint in the self-injected QD lasers independent of the cavity regime.

1 Introduction

Quantum-dot (QD) lasers have attracted lots of attention as the next generation laser sources for fibre telecommunication networks, because of promising properties such as low threshold current [1], temperature insensitivity [2], high bandwidth [3, 4] and low chirp [5, 6]. In particular, directly modulated lasers (DML) are expected to play a major role in the next generation telecommunication links for cooler-less and isolator-free applications. However, regarding the microwave properties, it has to be stressed that the QD DMLs have not yet fulfilled the expected dynamic requirements. Indeed, the maximum modulation bandwidth remains limited at room temperature to about 10–12 GHz (excluding the p-doping lasers and the tunneling injection lasers) at the optical fibre communication wavelength bands (1.3–1.6 μm) [7], which is much lower than the best reported values for the two-dimensional (2D) quantum well (QW) lasers [8]. Deeper investigations of the QD lasers properties are needed especially to understand the intrinsic limitations related to the QD physical properties. To ensure a lasing emission at 1.55 μm, InAs QDs are preferentially grown by molecular beam epitaxy (MBE) on the InP substrates [5]. To this end, depending on the InP crystallographic orientation, it is known that the shape of the nanostructures is altered. For instance, on InP(100), elongated quantum dashes are closer to the 1D nanostructures (so-called quantum wires) while those on InP(311B) are truly fully confined 0D quantum boxes with a density as high as 10^{11} cm^{-2}. In such a way, a series of journal papers have theoretically investigated both the static and the dynamic properties of the InAs/InP(311B) QD lasers by taking into account the electronic and the optical properties of the nanostructures [9–13]. Semi-empirical modelling of the InAs/InP QD lasers has indeed reached a high level of sophistication, close to the one used for the QW lasers [14]. The basic physical properties of the InAs/InP QD (size and shape distributions, strain and piezoelectric field, electronic levels, multi-excitonic properties, material gain and optical polarisation, respectively) were progressively studied over the years [15–19], exhibiting somewhat different features than the InAs/GaAs QD counterparts. Dynamic properties (exciton or biexciton radiation times, carrier injection from the wetting layer, relaxation Auger effect, tunneling effect through the excited states in the high density QDs and the electronic coupling of the QD layers, respectively) were especially explored by time-resolved photoluminescence or pump probe experiments [19–21]. The understanding of the static lasing properties (the optimisation of the threshold current, dual emission between the ground state (GS) and the first excited state (ES) and carrier redistribution at high temperature, respectively) has benefited from the combined experimental and theoretical studies. It was thus possible to explore theoretically the influence of some key physical parameters, such as carrier capture, relaxation times and the Pauli blocking factor, on the dynamic properties of the InAs/InP QD lasers operated at 1.55 μm [11–13]. New relationships for the resonance frequency and the damping factor as well as the modulation transfer function have been

demonstrated. The semi-empirical model has also recently opened the possibility to investigate the materials parameters controlling the non-linear photonic properties such as the stability diagram of the InAs/InP QD lasers operating under external controls (self-injection and optical injection) [12, 13]. In particular, it is well-known that the semiconductor lasers are highly sensitive to the parasitic reflections [22]. To this end, diode lasers exhibit very interesting non-linear dynamic features either leading to instabilities and chaotic behaviours or improving the device's intrinsic characteristics. Although Faraday isolators have been used extensively to reduce back reflections, the elimination of the optical isolator remains a big challenge and is still desirable for the low-cost applications [23]. In the view of future implementations of the QD lasers in the optical fibre links, studying the behaviour of such devices in the presence of optical feedback is of first importance. As a result, since the modulation of the gain and the optical index of the semiconductor medium leads to a severe shift in the resonant mode as well as to a broader optical spectrum, investigating the frequency chirp properties in the nanostructured lasers is relevant for designing long-distance and high-bit rate optical communications systems. Thus, the aim of this paper is to study the dynamic properties, especially the frequency chirp of the self-injected InAs/InP QD lasers by properly taking into account the fine structure of the semiconductor material, the linewidth enhancement factor (LEF) as well as the external cavity length. Although various approaches taking into account the peculiar characteristics of the self-injected QD lasers were previously reported in the literature [24, 25], those were mostly numerical and have not really investigated the frequency chirp properties of the laser. In addition, it is expected that the semi-analytical model proposed in this paper would provide new insights of the laser's dynamic characteristics via an easy identification of the key parameters controlling the frequency chirp.

The paper is organised as follows. In Section 2, the theoretical model used to analyse the dynamic characteristics of the self-injected QD lasers is presented. Starting from the laser's rate equations, it is shown that the small-signal analysis allows us to extract both the modulation response and the frequency chirp as well as successfully predict the key features of the self-injected oscillator. The novelty presented in the paper relies on a semi-analytical derivation, which directly incorporates the QD carrier dynamics as well as the non-linear gain. Section 3 presents the numerical results and discussions by taking into account the effects of the external cavity length and the LEF. The conclusions and outlooks are given in Section 4.

2 Semi-analytical model

Fig. 1 shows a basic scheme of the self-injected QD laser with L_{in} being the length of the laser cavity and L_{ex} being the length of the external cavity. The model commonly used to describe the dynamics of the semiconductor lasers with external optical feedback is the well-known Lang–Kobayashi (LK) model [26], in which a one rate equation describes the complex electric field (amplitude and phase) whereas the other one accounts for the carrier density. To take into account the complex carrier dynamics occurring in the QD lasers, Huyet *et al.* [27] coupled two additional carrier rate equations into the LK model namely one for the population in the wetting layer (WL) and one for the

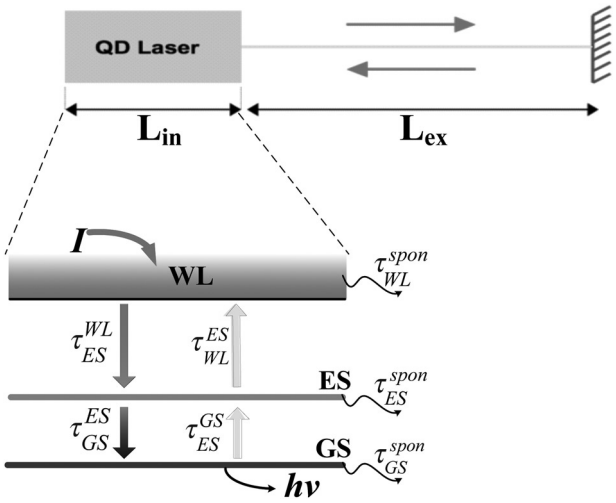

Fig. 1 *Basic scheme of the QD lasers operating under self-injection and a sketch of the corresponding carrier dynamics*

population in the dots in which the effects of the Auger carrier capture rate and the Pauli blocking effect were also analysed. To this end, it was shown that the insensitivity to the optical feedback of the QD lasers resulted from the low LEF and strongly damped relaxation oscillations. By employing a similar method, the bifurcation scenarios of the QD lasers with optical feedback were also studied in [28]. In this paper, the numerical model of the QD laser holds under the assumption that the active region consists of only one QD ensemble, where the nanostructures are interconnected by the WL. The QD ensemble includes two energy levels: a 2-fold degenerate GS and a 4-fold degenerate ES. The QDs are assumed to be always neutral in the excitonic energy states, where the electrons and the holes are treated as electron–hole (eh) pairs. As shown in Fig. 1, the carriers are firstly injected into the WL before being captured into the ES within a capture time τ_{ES}^{WL}, and then relax into the GS within a relaxation time τ_{GS}^{WL}. On the other hand, the carriers can also escape from the GS (τ_{ES}^{GS}) and ES (τ_{WL}^{ES}). A detailed balance principle is assumed to govern the carrier distribution dynamics even at a high modulation rate. After some further approximations as those described in [13], the QD laser with the optical feedback is described by the following set of differential rate equations

$$\frac{dN_{WL}}{dt} = \frac{I}{q} + \frac{N_{ES}}{\tau_{WL}^{ES}} - \frac{N_{WL}}{\tau_{ES}^{WL}} f_{ES} - \frac{N_{WL}}{\tau_{WL}^{spon}} \tag{1}$$

$$\frac{dN_{ES}}{dt} = \frac{N_{WL}}{\tau_{ES}^{WL}} f_{ES} + \frac{N_{GS}}{\tau_{ES}^{GS}} f_{ES} - \frac{N_{ES}}{\tau_{WL}^{ES}} - \frac{N_{ES}}{\tau_{GS}^{ES}} f_{GS} - \frac{N_{ES}}{\tau_{ES}^{spon}} \tag{2}$$

$$\frac{dN_{GS}}{dt} = \frac{N_{ES}}{\tau_{GS}^{ES}} f_{GS} - \frac{N_{GS}}{\tau_{ES}^{GS}} f_{ES} - \frac{N_{GS}}{\tau_{GS}^{spon}} - \Gamma_p g v_g S \tag{3}$$

$$\frac{dS}{dt} = \left(\Gamma_p g v_g - \frac{1}{\tau_p}\right) S + \beta_{SP} \frac{N_{GS}}{\tau_{GS}^{spon}} + 2k_c \sqrt{S(t)S(t-\tau_{ex})} \cos(\Delta\phi) \tag{4}$$

$$\frac{d\phi}{dt} = \frac{\alpha_H}{2}\left(\Gamma_p g v_g - \frac{1}{\tau_p}\right) - k_c \sqrt{\frac{S(t-\tau_{ex})}{S(t)}} \sin(\Delta\phi) \tag{5}$$

doi: 10.1049/iet-opt.2013.0078

where $N_{WL,\ ES,\ GS}$ are the carrier numbers in WL, ES and GS, respectively. The symbol S represents the number of the photons emitted from the GS while I is the pump current. The stimulated emission from the ES is not taken into account in the model. In (3)–(5) ϕ denotes the phase, β_{sp} the spontaneous emission factor, Γ_p the confinement factor, τ_p the photon lifetime, v_g the group velocity and α_H the LEF.

The GS gain is written as follows

$$g = \frac{a_{GS}\left(N_{GS} - N_B A_{sf}\right)/V_{QD}}{1 + \varepsilon S/V_p} \tag{6}$$

where a_{GS} is the differential gain, N_B is the QD surface density, A_{sf} is the surface area of the QDs. V_p is the photon volume, V_{QD} is the total volume of the QDs and ε accounts for the gain compression coefficient, respectively.

Besides, the Pauli blocking factors are given by

$$f_{GS} = 1 - \frac{N_{GS}}{2N_B}; \quad f_{ES} = 1 - \frac{N_{ES}}{4N_B} \tag{7}$$

The strength of the delayed field is defined as follows

$$k_c = \frac{1}{\tau_{in}} \frac{1 - R_1}{\sqrt{R_1}} \sqrt{f_{ext}} \tag{8}$$

where τ_{in} is the round trip time in the laser cavity, R_1 is the laser facet reflectivity and f_{ext} is the feedback ratio corresponding to the ratio of the returned power into the laser's facet to the emitted one.

The phase variation occurring in (4) and (5) is expressed as

$$\Delta\phi = \omega_0 \tau_{ex} + \phi(t) - \phi(t - \tau_{ex}) \tag{9}$$

with ω_0 the solitary laser frequency, and τ_{ex} the round trip delay in the external cavity. All the parameters used in the simulations are listed in Table 1, and correspond to those measured on a 1.52-μm InAs/InP (311B) QD laser [29]. Let us remark that the capture time τ_{ES}^{WL} and the relaxation time τ_{GS}^{ES} are both set at half the measured values so as to clearly show the variations of the damping rate in the following sections.

Table 1 List of all the laser parameters used in the simulations

Material and laser parameters		
Symbols	Definitions	Values
E_{WL}	WL energy	0.97 eV
E_{ES}	ES energy	0.87 eV
E_{GS}	GS energy	0.82 eV
τ_{ES}^{WL}	capture time from WL to ES	12.6 ps
τ_{GS}^{ES}	relaxation time from ES to GS	5.8 ps
τ_{WL}^{spon}	spontaneous time of WL	500 ps
τ_{ES}^{spon}	spontaneous time of ES	500 ps
τ_{GS}^{spon}	spontaneous time of GS	1200 ps
a_{GS}	differential gain	5×10^{-15} cm^2
ε	gain compression coefficient	5×10^{-16} cm^3
n_r	refractive index	3.5
L	active region length	0.05 cm
W	active region width	4×10^{-4} cm
N	number of QD layers	5
N_B	QD density	10×10^{10} cm^{-2}
Γ_p	optical confinement factor	0.06
β_{sp}	spontaneous emission factor	1×10^{-4}
α_i	internal modal loss	6 cm^{-1}
$R_1 = R_2$	facet reflectivity	0.32
L_{ex}	external cavity length	0.35, 105 cm
n_{ex}	refractive index in the external cavity	1.5
α_H	linewidth enhancement factor	1

To obtain the modulation properties, the rate equations can be linearised by a modified small-signal analysis [30]. On considering a sinusoidal current modulation $I_1 e^{j\omega t}$ around the injection current I_0, the following laser values also vary around their steady-state solutions as

$$\begin{aligned} I(t) &= I_0 + (I_1 e^{j\omega t} + \text{c.c.}) \\ S(t) &= S_0 + (S_1 e^{j\omega t} + \text{c.c.}) \\ \phi(t) &= \Delta\omega t + (\phi_1 e^{j\omega t} + \text{c.c.}) \\ N_{WL,ES,GS}(t) &= N_{WL0,ES0,GS0} + (N_{WL1,ES1,GS1} e^{j\omega t} + \text{c.c.}) \end{aligned} \tag{10}$$

with c.c. referring to the complex conjugate term. Inserting (10) into (1)–(5) and neglecting the higher order terms allows the derivation of the linearised rate equations with some Taylor polynomial approximations

$$\begin{bmatrix} \gamma_{11} + jw & -\gamma_{12} & 0 & 0 & 0 \\ -\gamma_{21} & \gamma_{22} + jw & -\gamma_{23} & 0 & 0 \\ 0 & -\gamma_{32} & \gamma_{33} + jw & -\gamma_{34} & 0 \\ 0 & 0 & -\gamma_{43} & \gamma_{44} + jw & -\gamma_{45} \\ 0 & 0 & -\gamma_{53} & -\gamma_{54} & \gamma_{55} + jw \end{bmatrix} \times \begin{bmatrix} N_{WL1} \\ N_{ES1} \\ N_{GS1} \\ S_1 \\ \phi_1 \end{bmatrix} = \frac{I_1}{q} \begin{bmatrix} 1 \\ 0 \\ 0 \\ 0 \\ 0 \end{bmatrix} \tag{11}$$

with

$$\gamma_{11} = \frac{f_{ES0}}{\tau_{ES}^{WL}} + \frac{1}{\tau_{WL}^{spon}} \quad \gamma_{12} = \frac{1}{\tau_{WL}^{ES}} + \frac{N_{WL0}}{4N_B \tau_{ES}^{WL}}; \quad \gamma_{21} = \frac{f_{ES0}}{\tau_{ES}^{WL}}$$

$$\gamma_{22} = \frac{f_{GS0}}{\tau_{GS}^{ES}} + \frac{1}{\tau_{WL}^{ES}} + \frac{N_{WL0}}{4N_B \tau_{ES}^{WL}} + \frac{1}{\tau_{ES}^{spon}}$$

$$\gamma_{23} = \frac{f_{ES0}}{\tau_{ES}^{GS}}$$

$$\gamma_{32} = \frac{f_{GS0}}{\tau_{GS}^{ES}}; \quad \gamma_{33} = \frac{f_{ES0}}{\tau_{ES}^{GS}} + \frac{1}{\tau_{GS}^{spon}} + \frac{\Gamma_p v_g a_{GS} S_0}{V_{QD}}; \quad \gamma_{34} = \frac{1}{\tau_p}$$

$$\gamma_{43} = \frac{\beta_{SP}}{\tau_{GS}^{spon}} + \Gamma_p v_g a_{GS} S_0 (1 - \varepsilon S_0/V_p)/V_{QD}$$

$$\gamma_{44} = -Pk_c(1 + e^{-j\omega\tau_{ex}}) + 2\frac{\varepsilon S_0}{\tau_p V_p}$$

$$\gamma_{45} = 2Pk_c\alpha_H S_0 (1 - e^{-j\omega\tau_{ex}})$$

$$\gamma_{53} = \frac{\alpha_H}{2}\Gamma_p v_g a_{GS}(1 - \varepsilon S_0/V_p)/V_{QD}$$

$$\gamma_{54} = -\frac{\alpha_H}{2}\frac{Pk_c}{S_0}(1 - e^{-j\omega\tau_{ex}}) - \frac{\alpha_H}{2}\frac{\varepsilon}{\tau_p V_p}$$

$$\gamma_{55} = Pk_c(1 - e^{-j\omega\tau_{ex}}) \quad (12)$$

with $P = 1/\sqrt{1+\alpha_H^2}$ while the relationship $\Gamma_p v_g a_{GS}(N_{GS0} - N_B) \simeq 1/\tau_p$ holds under the assumption of a weak optical feedback level. It is known that under a direct modulation, the strong non-linear photon–carrier coupling in a semiconductor laser cavity gives rise to both amplitude and frequency modulation responses. Thus, from (11), the amplitude modulation transfer function for the QD lasers subjected to external optical feedback can be extracted as

$$H(\omega) = \frac{S_1(\omega)/I_1(\omega)}{S_1(0)/I_1(0)} \quad (13)$$

The frequency response (frequency chirp) is evaluated via the chirp-to-power ratio (CPR) given by the expression

$$\mathrm{CPR} = \left|\frac{\Delta\omega}{\Delta S}\right| = \left|j\omega\frac{\phi_1(\omega)}{S_1(\omega)}\right| \quad (14)$$

The CPR is a convenient way to quantify the chirping properties as already demonstrated both theoretically and experimentally [30, 31]. In the following section, we investigate the effects of the feedback parameters on the modulation response and on the CPR properties both for the short and the long external cavity configurations. The influence of the LEF is also discussed.

3 Numerical results and discussion

In the following section, the bias current is set at $I_{bias} = 1.1 \times I_{th}$ with I_{th} being the threshold current of the free running laser (e.g. without the optical feedback). To avoid any detrimental feedback regime, the intensity of the delayed field re-entering into the laser cavity was always maintained below its critical value $f_{ext,c}$ [32]. This last assumption is particularly relevant in the long cavity regime in which severe instabilities such as coherence collapse can arise above this critical value (and even at moderate feedback rates) [33]. For instance, within the fully developed coherence collapse regime, the optical spectrum being significantly broadened, the capacity for high-speed communications is highly altered [31, 32]. Fig. 2*a* depicts the effect of a phase shift on the modulation responses in the short cavity regime for relatively high feedback levels of $f_{ext} = 10^{-2}$ and $\alpha_H = 1$, respectively. The phase term $\omega\tau_{ex}$ is varied by controlling the external cavity length such as $L_{ex} = 0.12$ cm ($\phi_0 = 2\pi \times 0.24$), $L_{ex} = 0.20$ cm ($\phi_0 = 2\pi \times 0.73$), $L_{ex} = 0.35$ cm ($\phi_0 = 2\pi \times 0.02$) and $L_{ex} = 0.43$ cm ($\phi_0 = 2\pi \times 0.51$), respectively. Gain compression is not taken into account at this stage in the calculations ($\varepsilon = 0$). As shown, the phase of the delayed field modifies the global shape of the modulation response and affects the key modulation features such as the relaxation peak and the bandwidth capacity. In the best configuration with $L_{ex} = 0.35$ cm, the simulations point out that the modulation bandwidth is improved by a factor of about 1.5 up to 12 GHz. Since the short external cavity always leads to a stable regime for any large feedback level, the bandwidth can be certainly further enhanced by increasing the feedback strength or by shortening the external cavity length [34]. In contrast, Fig. 2*b* compares the modulation response between the short and the long cavity configurations by assuming a moderate feedback level of $f_{ext} = 10^{-3}$. The simulations demonstrate that the long cavity regime is not favourable for improving the modulation properties. Ripples (zoomed figure in the inset) appear in the modulation response, and the periodicity of the oscillation is fixed by the round trip time of the external cavity. If both the feedback rate and the LEF are too large, the magnitude of the ripple leads to a substantial overshoot in the modulation response [13].

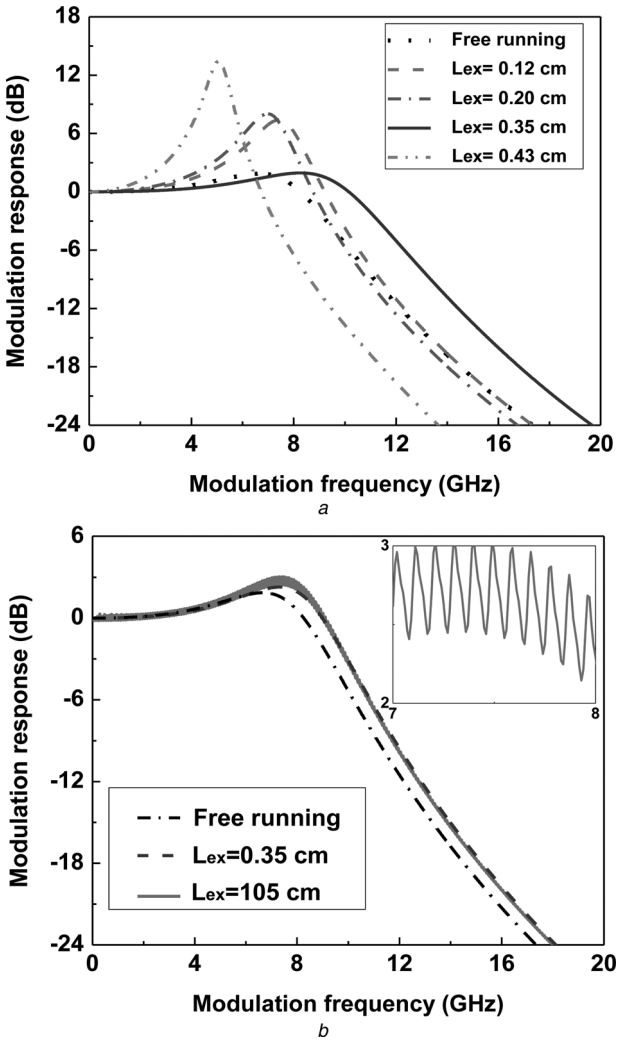

Fig. 2 *Calculated amplitude modulation response*

a Short external cavity regime ($f_{ext} = 10^{-2}$, $\varepsilon = 0$)
b Long external cavity regime ($f_{ext} = 10^{-3}$)
Phase term $\omega\tau_{ex}$ is varied by controlling the external cavity length $L_{ex} = 0.12$ cm ($\phi_0 = 2\pi \times 0.24$), $L_{ex} = 0.20$ cm ($\phi_0 = 2\pi \times 0.73$), $L_{ex} = 0.35$ cm ($\phi_0 = 2\pi \times 0.02$) and $L_{ex} = 0.43$ cm ($\phi_0 = 2\pi \times 0.51$), respectively

Fig. 3*a* shows the CPR calculated under the short cavity regime for various feedback levels ranging from 10^{-5} to 10^{-2}. To study the frequency response, the gain compression factor ε which incorporates complex phenomena such as the spectral hole burning and the carrier heating is maintained at a constant value of 5×10^{-16} cm^3 [7]. Let us also note that the thermal chirp which typically occurs for modulation frequencies below 0.01 GHz is not

doi: 10.1049/iet-opt.2013.0078

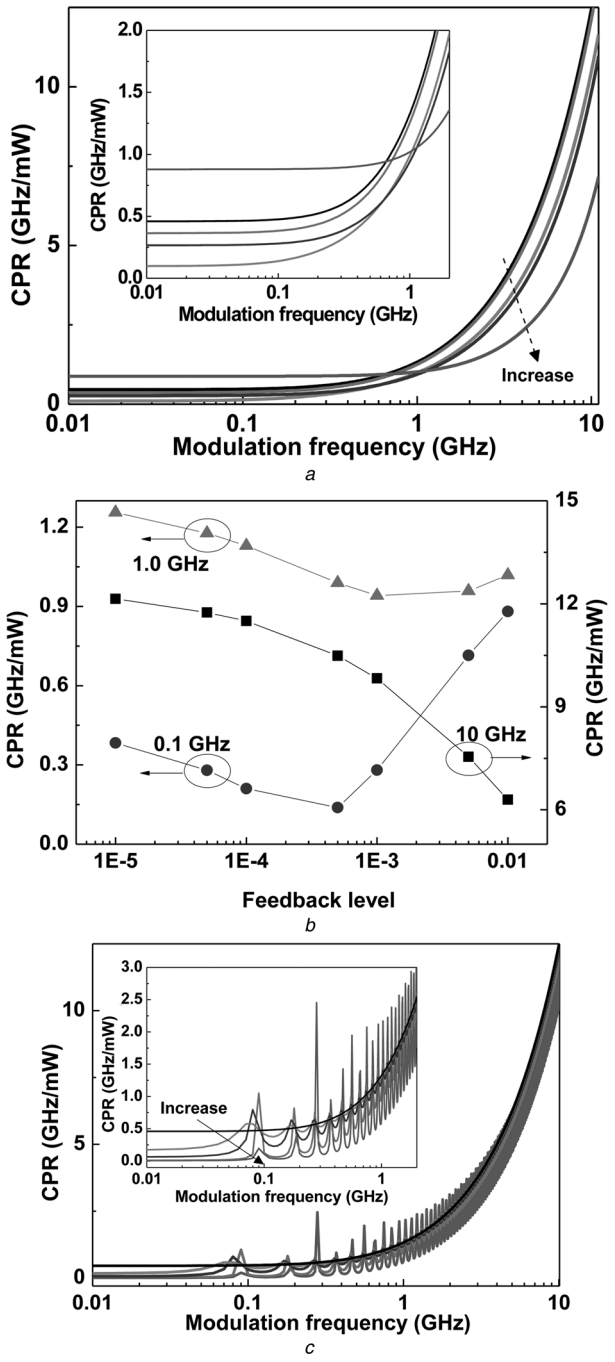

Fig. 3 *Calculated CPR for various optical feedback conditions*

a Calculated CPR in the short cavity regime ($L_{ex} = 0.35$ cm and $\varepsilon = 5 \times 10^{-16}$ cm^3) with f_{ext} increasing from 0, 10^{-5}, 5×10^{-4}, 10^{-3} to 10^{-2}

b Calculated CPR in the short cavity regime ($L_{ex} = 0.35$ cm and $\varepsilon = 5 \times 10^{-16}$ cm^3) as a function of the optical feedback level for the modulation frequencies of 0.1, 1.0 and 10 GHz, respectively

c Calculated CPR in the long cavity regime ($L_{ex} = 105$ cm and $\varepsilon = 5 \times 10^{-16}$ cm^3) with f_{ext} increasing from 0, 10^{-6}, 10^{-5}, 10^{-4} and to 10^{-3}

included in the model. Consequently, all the simulations are performed by assuming modulation frequencies varying from 0.01 to 10 GHz. As a result, when the modulation frequency ranges from 0.01 to 1 GHz, the thermal effects are no longer significant compared with the refractive index ones induced by the modulation of the carrier density. In such a way, the semiconductor laser evolves within the adiabatic regime with the in-phase (AM) and (FM) responses. In this regime, the adiabatic CPR is relatively independent of the modulation frequency, but does remain sensitive to the optical feedback conditions. Indeed, as discussed hereafter, increasing the amplitude of the delay term can result in either an improvement or a degradation of the CPR. Then, for modulation frequencies larger than 1 GHz, a transient regime occurs giving rise to crossed relaxation oscillations between the carrier and the photon numbers in the laser's cavity. Although the CPR enhances monolithically with the modulation frequency, it can be nicely reduced by increasing the strength of the external control. To summarise the previous statements, Fig. 3*b* shows a superposition of the calculated CPR as a function of the feedback level for the three modulation frequencies of 0.1, 1 and 10 GHz, respectively. As stated previously, within the adiabatic regime, the CPR can behave differently since it can decrease with the feedback strength until a minimum and then reincreases afterwards. Thus, in the case of a 0.1 GHz modulation frequency, the CPR is lowered from 0.40 GHz/mW ($f_{ext} = 10^{-5}$) to 0.13 GHz/mW ($f_{ext} = 5 \times 10^{-4}$) while it reincreases up to 0.9 GHz/mW at the highest feedback level ($f_{ext} = 10^{-2}$). This effect is lessened when the modulation frequency is located at the edge of the adiabatic regime. For instance, in Fig. 3*b*, for a 1 GHz modulation frequency, the CPR varies from 1.25 GHz/mW ($f_{ext} = 10^{-5}$) down to 1.0 GHz/mW for ($f_{ext} = 10^{-3}$) but remains roughly constant at the larger feedback level values. Finally, when the laser operates in the relaxation oscillation regime, the transient frequency chirp is purified. Thus, in the case of a 10 GHz modulation frequency, the CPR decreases by a factor of 2 from 12 GHz/mW ($f_{ext} = 10^{-5}$) down to 6 GHz/mW ($f_{ext} = 10^{-2}$). Fig. 3*c* shows the situation simulated for the long external cavity regime assuming various feedback levels ranging from 10^{-6} to 10^{-3}. Similar to the modulation response case, the long cavity regime produces parasitic peaks related to the number of the external cavity modes. When the laser operates within the adiabatic regime, it is however rather interesting to note that with a modulation frequency less than about 0.2 GHz, increasing the feedback level allows us to reduce both the amplitude of the parasitic peaks and the CPR. For instance, at a 0.1 GHz modulation frequency, the latter is lowered from 0.5 GHz/mW in the free-running case down to 0.1 GHz/mW ($f_{ext} = 10^{-3}$). These numerical results are actually in agreement with the recent experimental observations conducted on a QW distributed feedback laser in which the CPR was decreased in the adiabatic regime with a proper external control [31]. On the contrary, when the modulation frequency approaches the laser's relaxation frequency, the magnitude of the peaks is progressively enhanced especially under strong feedback rates.

Finally, the influence of the so-called phase amplitude coupling on the CPR response is studied both for the short (Fig. 4*a*) and the long cavity regimes (Fig. 4*b*). Simulations are conducted by assuming a constant feedback rate of 10^{-3} for the short cavity regime and 10^{-4} for the long cavity regime while the LEF is varied from 0.5 to 5.0. These variations typically correspond to the measured LEF values observed in the QD lasers in which this intrinsic laser's parameter is not necessarily reduced as compared with their QW laser counterparts. This limitation is attributed to the material systems and the competition between the bound states as well as the carrier filling in the non-lasing energy levels. In the short cavity regime, beyond a certain modulation frequency (>1 GHz), the simulations reveal that any increase of the phase–amplitude coupling in the laser's cavity results in a detrimental degradation of the CPR value. For instance, at a modulation frequency of 10 GHz,

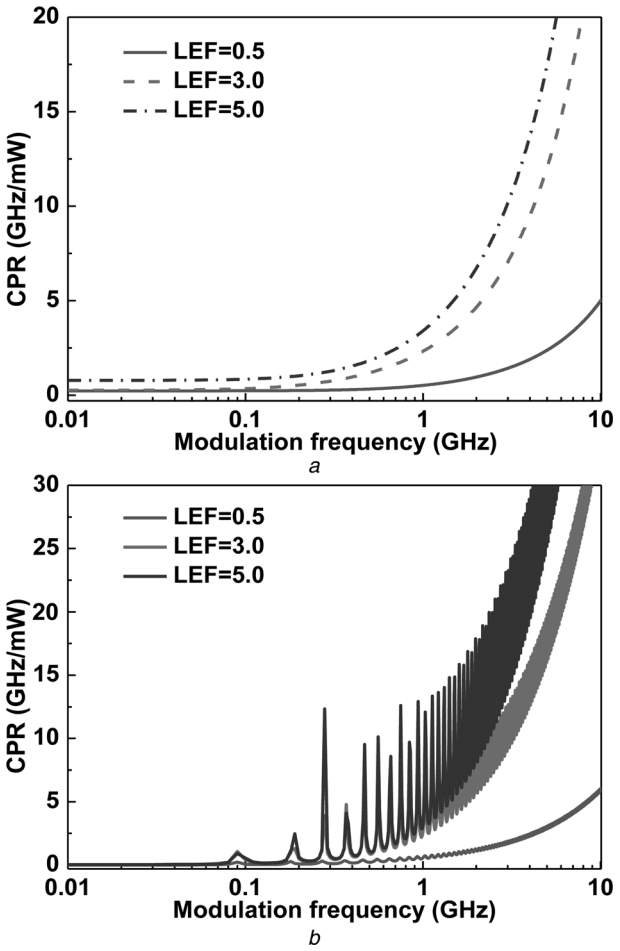

Fig. 4 *Calculated CPR for various values of the LEF ($0.5 < \alpha_H < 5.0$)*

a Short cavity regime ($L_{ex} = 0.35$ cm, $f_{ext} = 10^{-3}$ and $\varepsilon = 5 \times 10^{-16}$ cm^3, respectively)

b Long cavity regime ($L_{ex} = 105$ cm, $f_{ext} = 10^{-4}$ and $\varepsilon = 5 \times 10^{-16}$ cm^3, respectively)

the transient chirp is enhanced from 5 GHz/mW to more than 20 GHz/mW. The calculations also point out that the degradation of the CPR is even accelerated under the long cavity regime where the magnitude of the parasitic oscillations scales not only with the feedback rate but also with the LEF. Although the effect of the LEF on the CPR was originally reported in the QW based self-injected lasers [30], we believe that this phenomenon is much more predominant with the QD materials because larger variations of this parameter are usually reported from chip to chip.

4 Conclusion

As a conclusion, the presented results give insights for the analysis of the QD lasers in the presence of the optical feedback. As for the QW ones, the long delay case does not lead to the improvement of the modulation properties. Detrimental parasitic ripples whose magnitudes are scaled with the LEF clearly occur. On the contrary, the short cavity situation can be leveraged to our benefit to improve the modulation properties of the diode laser. To this end, depending on the amplitude and on the phase of the delayed field, great improvements in the device properties operating under direct modulation can be achieved including a larger modulation bandwidth, a higher relaxation frequency, a reduced non-linear distortion as well as lower adiabatic and transient chirps. However, the simulations also demonstrate that the LEF does constitute a severe constraint in the self-injected QD laser. Even under the short cavity regime a larger value of the phase–amplitude coupling factor can counteract all the positive effects from the optical feedback. The use of external optical feedback can be powerful since it relies on a simple, compact and cheap solution, which can be implemented in designing long-distance and high bitrate optical communications system as well as in future integrated photonic circuits.

5 Acknowledgments

Dr. Frédéric Grillot's work is supported by the European Office of Aeorospace Research and Development (EOARD) under grant number FA8655-12-1-2093. Cheng Wang's work is supported by the China Scholarship Council.

6 References

1 Liu, G.T., Stintz, A., Li, H., Malloy, K.J., Lester, L.F.: 'Extremely low room-temperature threshold current density diode lasers using InAs dots in In GaAs quantum well', *Electron. Lett.*, 1999, **35**, (14), pp. 1163–1165

2 Mikhrin, S.S., Kovsh, A.R., Krestnikov, I.L., *et al.*: 'High power temperature-insensitive 1.3 μm InAs/InGaAs/GaAs quantum dot lasers', *Semicond. Sci. Technol.*, 2005, **20**, (5), pp. 340–342

3 Mi, Z., Bhattacharya, P., Fathpour, S.: 'High-speed 1.3 μm tunnel injection quantum-dot lasers', *Appl. Phys. Lett.*, 2005, **86**, (15), pp. 153109

4 Kuntz, M., Fiol, G., Lammlin, M., *et al.*: '10 Gbit/s data modulation using 1.3 μm InGaAs quantum dot lasers', *Electron. Lett.*, 2005, **41**, (5), pp. 244–245

5 Saito, H., Nishi, K., Kamei, A., Sugou, S.: 'Low chirp observed in directly modulated quantum dot lasers', *IEEE Photon Technol. Lett.*, 2000, **12**, (10), pp. 1298–1300

6 Ghosh, S., Pradhan, S., Bhattacharya, P.: 'Dynamic characteristics of high-speed In0.4Ga0.6As/GaAs self-organized quantum dot lasers at room temperature', *Appl. Phys. Lett.*, 2002, **81**, (16), pp. 3055–3057

7 Grillot, F., Dagens, B., Provost, J.G., Su, H., Lester, L.F.: 'Gain compression and above-threshold linewidth enhancement factor in 1.3 μm InAs-GaAs quantum dot lasers', *IEEE J. Quantum Electron.*, 2008, **44**, (10), pp. 946–951

8 Fiore, A., Markus, A.: 'Differential gain and gain compression in quantum-dot lasers', *IEEE J. Quantum Electron.*, 2007, **43**, (3), pp. 287–294

9 Veselinov, K., Grillot, F., Cornet, C., *et al.*: 'Analysis of the double laser emission occurring in 1.55-μm InAs–InP (113)B quantum-dot lasers', *IEEE J. Quantum Electron.*, 2007, **43**, (9), pp. 810–816

10 Grillot, F., Veselinov, K., Gioannini, M., *et al.*: 'Spectral analysis of 1.55 μm InAs–InP(113)B quantum-dot lasers based on a multipopulation rate equations model', *IEEE J. Quantum Electron.*, 2009, **45**, (7), pp. 872–878

11 Wang, C., Grillot, F., Even, J.: 'Impacts of wetting layer and excited states on the modulation response of quantum-dot lasers', *IEEE J. Quantum Electron.*, 2012, **48**, (9), pp. 1144–1150

12 Wang, C., Grillot, F., Even, J.: 'Impacts of carrier capture and relaxation rates on the modulation response of injection-locked quantum dot lasers', *Photonic West, Phys. Simul. Optoelectron. Dev. XXI*, 2013, **8619**, pp. 861908

13 Grillot, F., Wang, C., Naderi, N.A., Even, J.: 'Modulation properties of self-injected quantum dot semiconductor diode lasers', *IEEE J. Sel. Top. Quantum Electron.*, 2013, **19**, (4), pp. 1900812

14 Coldren, L.A., Corzine, S.W.: 'Diode lasers and photonic integrated circuits' (Wiley, New York, 1995)

15 Cornet, C., Schliwa, A., Even, J., *et al.*: 'Theoretical investigation of electronic and optical properties of InAs/InP quantum dots on InP (100) and (311)B substrates', *Phys. Rev. B*, 2006, **74**, pp. 035312

16 Cornet, C., Levallois, C., Caroff, P., *et al.*: 'Increasing of charge redistribution efficiency in a laterally organized superlattice of coupled quantum dots', *Phys. Rev. B*, 2006, **74**, (24), pp. 245315

doi: 10.1049/iet-opt.2013.0078

17 Cornet, C., Labbe, C., Folliot, H., *et al*.: 'Quantitative investigations of optical absorption in InAs/InP (311)B quantum dots emitting at 1.55 μm wavelength', *Appl. Phys. Lett.*, 2004, **85**, (23), pp. 5685

18 Homeyer, E., Piron, R., Grillot, F., *et al*.: 'Demonstration of a low threshold current in 1.54 μm InAs/InP(311)B quantum dot laser with reduced quantum dot stacks', *Jap. J. Appl. Phys.*, 2007, **46**, pp. 6903

19 Cornet, C., Labbe, C., Folliot, H., *et al*.: 'Time-resolved pump-probe in 1.55-μm InAs/InP quantum dots under high resonant excitation', *Appl. Phys. Lett.*, 2006, **88**, (27), pp. 171502

20 Miska, P., Even, J., Dehaese, O., Marie, X.: 'Carrier relaxation dynamics in InAs/InP quantum dots', *Appl. Phys. Lett.*, 2008, **92**, (19), pp. 191103

21 Miska, P., Even, J., Marie, X., Dehaese, O.: 'Electronic structure and carrier dynamics in InAs/InP double-cap quantum dot', *Appl. Phys. Lett.*, 2009, **94**, (6), pp. 061916

22 Kane, D.M., Shore, K.A.: 'Unlocking dynamical diversity' (Wiley, New York, 2005)

23 Grillot, F., Thedrez, B., Py, J., Gauthier-Lafaye, O., Voiriot, V., Lafragette, J.L.: '2.5 Gbit/s transmission characteristics of 1.3 μm DFB lasers with external optical feedback', *IEEE Photon Technol. Lett.*, 2002, **14**, (1), pp. 101–103

24 Gioannini, M., Thé, G.A.P., Montrosset, I.: 'Multi-population rate equation simulation of quantum dot semiconductor lasers with feedback'. Int. Conf. on Numerical Simulation of Optoelectronic Devices, 2008, pp. 101–102

25 Otto, C., Lüdge, K., Viktorov, E., Erneux, T.: 'Quantum dot laser tolerance to optical feedback', *Nonlinear Laser Dyn., QD Cryptogr.*, 2011, Chapter 6, pp. 139–158

26 Lang, R., Kobayashi, K.: 'External optical feedback effects on semiconductor injection laser properties', *IEEE J. Quantum Electron.*, 1980, **16**, (3), pp. 347–355

27 Huyet, G., Brien, D.O., Hegary, S.P., *et al*.: 'Quantum dot semiconductor lasers with optical feedback', *Phys. Status Solidi. A*, 2004, **201**, (2), pp. 345–352

28 Otto, C., Lüdge, K., Schöll, E.: 'Modelling quantum dot lasers with optical feedback: sensitivity of bifurcation scenarios', *Phys. Status Solidi B*, 2010, **247**, (4), pp. 829–845

29 Martinez, A., Merghem, K., Bouchoule, S., *et al*.: 'Dynamic properties of InAs/InP(311B) quantum dot Fabry-Perot lasers emitting at 1.52 μm', *Appl. Phys. Lett.*, 2008, **93**, (2), pp. 021101

30 Duan, G.H., Gallion, P., Debarge, G.: 'Analysis of frequency chirping of semiconductor lasers in the presence of optical feedback', *Opt. Letts.*, 1987, **12**, (10), pp. 800–802

31 Kechaou, K., Grillot, F., Provost, J.-G., Thedrez, B., Erasme, D.: 'Self-injected semiconductor distributed feedback lasers for frequency chirp stabilization', *Opt. Express*, 2012, **20**, (23), pp. 26062–26074

32 Helms, J., Petermann, K.: 'A simple analytical expression for the stable operation range of laser diodes with optical feedback', *IEEE J. Quantum Electron.*, 1990, **26**, (5), pp. 833–836

33 Lenstra, D., Verbeek, B.H., den Boef, A.J.: 'Coherence collapse in single mode semiconductor lasers due to optical feedback', *IEEE J. Quantum Electron.*, 1985, **21**, (6), pp. 674–679

34 Radziunas, M., Glitzky, A., Bandelow, U., *et al*.: 'Improving the modulation bandwidth in semiconductor lasers by passive feedback', *IEEE J. Sel. Top. Quantum Electron.*, 2007, **13**, (1), pp. 136–142